Astron. Astrophys. 335, 510–516 (1998)

ASTRONOMY AND ASTROPHYSICS

Hot UV bright stars in globular clusters⋆

S. Moehler[1,2], **W. Landsman**[3], **and R. Napiwotzki**[1]

[1] Dr. Remeis-Sternwarte, Astronomisches Institut der Universität Erlangen-Nürnberg, Sternwartstrasse 7, D-96049 Bamberg, Germany
[2] Space Telescope Science Institute, 3700 San Martin Drive, Baltimore, MD 21218, USA
[3] Raytheon STX, NASA/GSFC, Greenbelt, MD 20770, USA

Received 19 February 1998 / Accepted 1 April 1998

Abstract. We have obtained medium-resolution spectra of seven UV-bright stars discovered on images of four southern globular clusters obtained with the Ultraviolet Imaging Telescope (UIT). Effective temperatures, surface gravities and helium abundances are derived from LTE and non-LTE model atmosphere fits. Three of the stars have sdO spectra, including M4-Y453 ($T_{\rm eff}$ = 58800 K, $\log g$ = 5.15), NGC 6723-III60 ($T_{\rm eff}$= 40600 K, $\log g$ = 4.46) and NGC 6752-B2004 ($T_{\rm eff}$ = 37000 K, $\log g$ = 5.25). All seven stars lie along either post-extended horizontal branch (EHB) or post-early AGB evolutionary tracks. The post-early AGB stars show solar helium abundances, while the post-EHB stars are helium deficient, similar to their EHB progenitors.

Key words: stars: Post-AGB – globular clusters: individual: NGC 2808; NGC 6121; NGC 6723; NGC 6752 – ultraviolet: stars

1. Introduction

Ultraviolet images of globular clusters are often dominated by one or two hot, luminous, "UV-bright" stars. The most luminous of these stars are believed to be post-asymptotic giant branch (post-AGB) stars, which go through a luminous UV-bright phase as they leave the AGB and move rapidly across the HR diagram toward their final white dwarf state. Despite their short lifetimes ($\sim 10^5$ yrs), hot post-AGB stars can dominate the total ultraviolet flux of an old stellar population. In particular, hot post-AGB stars probably make a significant (although not the dominant) contribution to the UV-upturn observed in elliptical galaxies (Brown et al. 1997). However, a large uncertainty exists in modeling the contribution of hot post-AGB stars to the integrated spectrum of an old stellar population, due to the strong dependence of the post-AGB luminosity and lifetime on the core mass, which in turn depends on when the stars leave the AGB (Charlot et al. 1996). Also the previous mass loss on the red giant branch (RGB) plays an important rôle here, since it determines the fate of a star during and after the horizontal branch stage: Stars with very low envelope masses settle along the extended horizontal branch (EHB) and evolve from there directly to the white dwarf stage, whereas stars with envelope masses of more than 0.02 $M_\odot$will at least partly ascend the AGB. A further uncertainty arises because theoretical post-AGB tracks have been only minimally tested for old, low-mass stars.

The last census of hot post-AGB stars in globular clusters was published by de Boer (1987), but this list is certainly incomplete. The detection of hot post-AGB stars in optical color-magnitude diagrams (CMD's) is limited by selection effects due to crowding in the cluster cores and to the large bolometric corrections for these hot stars. More complete searches are possible for hot post-AGB stars in planetary nebulae, for example, by using O III imaging. However, only four planetary nebulae (PNe) were discovered in a recent survey of 133 globular clusters (Jacoby et al. 1997), of which two were previously known (K648 in M 15, and IRAS 18333-2357 in M 22). Jacoby et al. expected to find 16 planetary nebulae in their sample, on the basis of the planetary nebula luminosity function for metal-poor populations. The origin of this discrepancy is not yet understood, but we mention two possible contributing factors. First, the O III search of Jacoby et al. may have missed some old, faint planetary nebulae. Second, Jacoby et al. derive the number of expected PNe from the total cluster luminosity, assuming that all stars in a globular cluster will eventually go through the AGB phase. But in a cluster such as NGC 6752, about 30% of the HB population consists of EHB stars (with $T_{\rm eff} > 20{,}000$ K), which are predicted to evolve into white dwarfs without ever passing through the thermally pulsing AGB phase. The exact fraction of stars which follow such evolutionary paths will depend on the poorly known mass loss rates during the HB and early-AGB phases.

While globular clusters with a populous EHB are expected to be deficient in post-AGB stars, they should show a substantial population of less luminous ($1.8 < \log L/L_\odot < 3$) UV-bright stars, which can be either post-EHB stars or post-early AGB stars. The population of post-EHB stars is expected to be about 15–20 % of the population of EHB stars (Dorman et al. 1993). The post-early AGB population arises from hot HB stars with sufficient envelope mass to return to the AGB, but which peel off the AGB prior to the thermally pulsing phase (Dorman et al. 1993).

Send offprint requests to: S. Moehler

⋆ Based on observations collected at the European Southern Observatory (ESO N° 57.E-0101)

During the two flights of the *ASTRO* observatory in 1990 and 1995, the Ultraviolet Imaging Telescope (UIT, Stecher et al. 1997) was used to obtain ultraviolet ($\sim$ 1600 Å) images of 14 globular clusters. The solar-blind detectors on UIT suppress the cool star population, which allows UV-bright stars to be detected into the cluster cores, and the $40'$ field of view of UIT is large enough to image the entire population of most of the observed clusters. Thus, the UIT images provide a complete census of the hot UV-bright stars in the observed clusters. We have begun a program to obtain spectra of all the UV-bright stars found on the UIT images, in order to derive effective temperatures and gravities for the complete sample, for comparison with evolutionary tracks. Several of the UV-bright stars found on the UIT images, such as ROB 162 in NGC 6397, Barnard 29 in M 13, and vZ 1128 in M 3, were previously known and are well-studied. Other UIT stars are too close to the cluster cores for ground-based spectroscopy, and will require HST observations for further study. In this paper, we report on spectroscopy of those UIT UV-bright stars accessible for ground-based observations from the southern hemisphere.

2. Observations

In May 1996 we took medium resolution spectra of UV bright stars in southern globular clusters using EFOSC2 at the 2.2m MPI/ESO telescope (Table 1). We used grism #3 (100 Å/mm, 3800 – 5000 Å) and a slit width of $1''$, resulting in a resolution of 6.7 Å. The instrument was equipped with a Thompson CCD (19μm pixel size, 1024 $\times$ 1024 pixels, gain 2.1 e^-/ADU, readout-noise 4.3 e^-). For calibration purposes we always observed 10 bias frames each night and 5-10 flat-fields with a mean exposure level of about 10000 ADU each. For observations longer than 30 minutes we took wavelength calibration frames before and after the object's observation. Since the Ar light is rather faint, we took HeAr frames at the beginning of the night and only He during the night. The seeing values and slit orientations are listed in Table 1.

3. Data reduction

We averaged the bias frames over all nights of the run, as they showed no deviations above the 1% level. For the bias correction we added the difference in the mean overscans of the science and the bias frame to the mean bias frame, which was then subtracted from the science frame. We did not correct for dark current, which was less than 3 cts/hr/pix and showed no discernible structure. The flat fields were averaged separately for each night and normalized by dividing them by a smoothed average along the spatial axis. The flat fields showed night-to-night variations of less than 1% between the first and second night and again between the third and fourth night. We therefore averaged the flat-fields of the first and second night and those of the third and fourth night.

For the wavelength calibration we used a $3^{\rm rd}$ order polynomial to fit the dispersion relation for the HeAr frames. We used 15 lines, avoiding blended lines. The fits then yielded mean residuals of less than 0.2 Å. From the He frames obtained during the night we derived offsets relative to the HeAr frames by cross correlating the spectra, which were then used to adjust the zero-points of the dispersion relations.

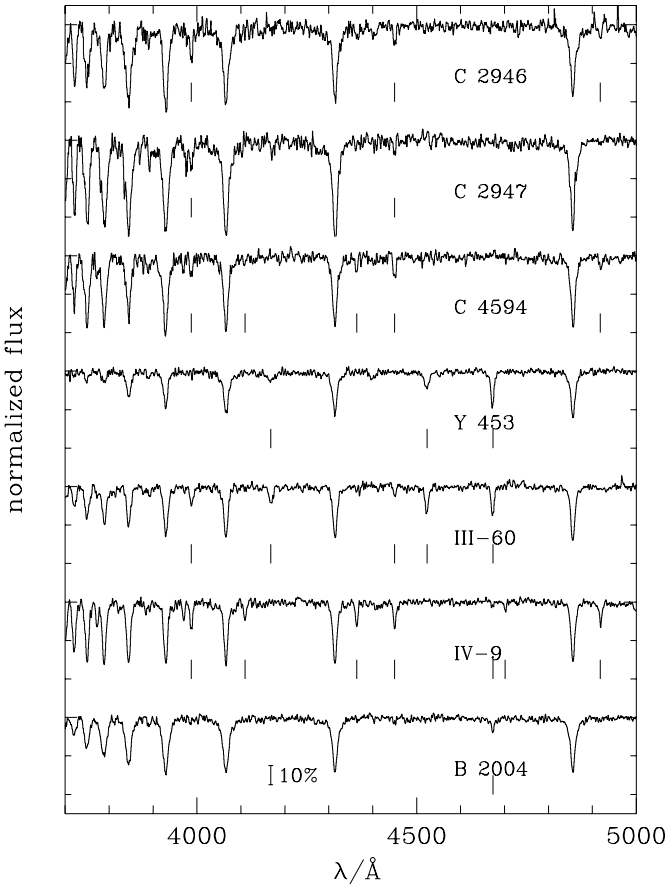

Fig. 1. The normalized spectra of the UV bright stars. The He I and He II absorption lines are marked.

We rebinned the frames two-dimensionally to constant wavelength steps. Before the sky fit the frames were median filtered along the spatial axis to remove cosmic rays in the background. To determine the sky background we had to find regions not containing any stellar spectra, which were sometimes distant from the object's location. Nevertheless the flat field correction and wavelength calibration turned out to be good enough that a constant fit to the spatial distribution of the sky light allowed us to subtract the sky background at the object's position with sufficient accuracy in the less crowded regions of the globular clusters, i.e. we do not see any absorption lines caused by the predominantly red stars of the clusters or by moon light. For those stars that lay closer to the cluster center the background light of the cluster showed a gradient across the frame and we therefore used a linear fit for the spatial distribution of the background light. The fitted sky background was then subtracted from the unsmoothed frame and the spectra were extracted using Horne's algorithm (Horne, 1986) as implemented in MIDAS.

The normalized spectra are plotted in Fig. 1. Spectra of the UV-bright stars ROA 542 and ROA 3596 in ω Cen obtained during

Table 1. List of observed stars and observing parameters

Cluster	Star	α_{2000}	δ_{2000}	V [mag]	B−V [mag]	slit orientation	seeing [″]
NGC 2808	C2946[1]	$09^h12^m22^s.36$	-64°52′37″.3	17.63	+0.09	EW/NS	1.0 – 1.9
	C2947[1]	$09^h12^m22^s.86$	-64°52′36″.7	17.10	+0.21	EW/NS	1.0 – 1.9
	C4594[1]	$09^h12^m01^s.98$	-64°47′35″.1	16.36	+0.03	NS	1.6 – 1.9
NGC 6121	Y453[2]	$16^h23^m22^s.25$	-26°28′02″.4	15.86	+0.00	NS	1.0 – 1.4
NGC 6723	III-60[3]	$18^h59^m29^s.0$	-36°40′49″.0	15.61	−0.25	NS	2.6 – 3.9
	IV-9[3]	$18^h59^m24^s.1$	-36°37′56″.0	14.64[4]	−0.17[4]	EW	1.5 – 1.6
NGC 6752	B2004[5]	$19^h11^m04^s.9$	-59°57′47″.0	16.42	−0.31	EW/NS	1.2 – 1.7

[1] Ferraro et al. (1990) (This photometry has been adjusted 0.1 mag fainter, as reported by Sosin et al., 1997)
[2] Cudworth & Rees (1990)
[3] Menzies (1974)
[4] L.K. Fullton (priv. comm.)
[5] Buonanno et al. (1986)

this run will be reported in a separate paper (Landsman et al. 1998).

4. Spectroscopic analyses

To derive effective temperatures, surface gravities and helium abundances we fitted the observed Balmer and helium lines with appropriate stellar model atmospheres. Beforehand we corrected the spectra for radial velocity shifts, derived from the positions of the Balmer and helium lines. The resulting heliocentric velocities are listed in Table 2, together with the physical parameters of the stars. To establish the best fit we used the routines developed by Bergeron et al. (1992) and Saffer et al. (1994), which employ a χ^2 test.

4.1. Subdwarf O stars

Those stars which show He II lines in their spectra (Y453 in NGC 6121, III-60 in NGC 6723, and B2004 in NGC 6752) are classified as sdO stars. To analyse these stars correctly it is necessary to take non-LTE effects into account. NLTE model atmospheres were calculated with the code developed by Werner (1986). The basic assumptions are those of static, plane-parallel atmospheres in hydrostatic and radiative equilibrium. In contrast to the ATLAS9 atmospheres used to analyse the cooler programme stars, we relax the assumption of local thermal equilibrium (LTE) and solve the detailed statistical equilibrium instead. The accelerated lambda iteration (ALI) method is used to solve the non-linear system of equations as described in Werner (1986).

To keep the computational effort within reasonable limits we neglected the influence of heavy elements and assumed a mixture of hydrogen and helium only. Elaborate hydrogen and helium model atoms were used for this purpose and pressure dissolution of the higher levels is included according the Hummer & Mihalas (1988) occupation probability formalism. Details are given in Napiwotzki (1997). Our NLTE model grid covers the temperature range $27000 < \mathrm{T_{eff}} < 70000$ K (stepsize increasing with $\mathrm{T_{eff}}$ from 2000 K to 5000 K) and gravity range $3.5 < \log \mathrm{g} < 7.0$ (stepsize 0.25 dex) with the helium abundance varying from $\log \frac{\mathrm{n_{He}}}{\mathrm{n_H}} = -3.0$ to $+0.5$ in 0.5 dex steps. The fits for the parameters given in Table 2 are shown in Fig. 2.

4.2. Cooler UV bright stars

The remaining stars showed only Balmer and He I lines in their spectra. For these stars LTE model atmospheres are sufficient to derive physical parameters (Napiwotzki 1997). We computed model atmospheres using ATLAS9 (Kurucz 1991, priv. comm.) and used the LINFOR program (developed originally by Holweger, Steffen, and Steenbock at Kiel university) to compute a grid of theoretical spectra, which include the Balmer lines H_α to H_{22} and He I lines. The grid covered the range 10000 ... 27500 K in $\mathrm{T_{eff}}$, 2.5 ... 5.0 in $\log \mathrm{g}$ and −2.0 ... −0.3 in $\log \frac{\mathrm{n_{He}}}{\mathrm{n_H}}$ at metallicities of −2 and −1 (Lemke, priv. comm.).

We fitted the Balmer lines from H_β to H_{12} (excluding H_9 because of the interstellar Ca II H line) and (if present) the He I lines $\lambda\lambda$ 4026 Å, 4388 Å, 4472 Å, 4922 Å, and 5016 Å. Fitting the spectra of the three stars in NGC 2808 and IV-9 in NGC 6723 with models for both metallicities resulted in temperature differences of about 500 K (the temperature being higher for the lower metallicity). The surface gravities and helium abundances were not affected. We decided to keep the values determined for a metallicity of −1.0, since this value is closer to the actual metallicities of these two clusters. The results of the spectroscopic analyses are given in Table 2.

5. Luminosities and masses

To compute the luminosities, we require the cluster distances and reddenings. These values are taken from the May 1997 tabulation of Harris (1996) except that the distance and

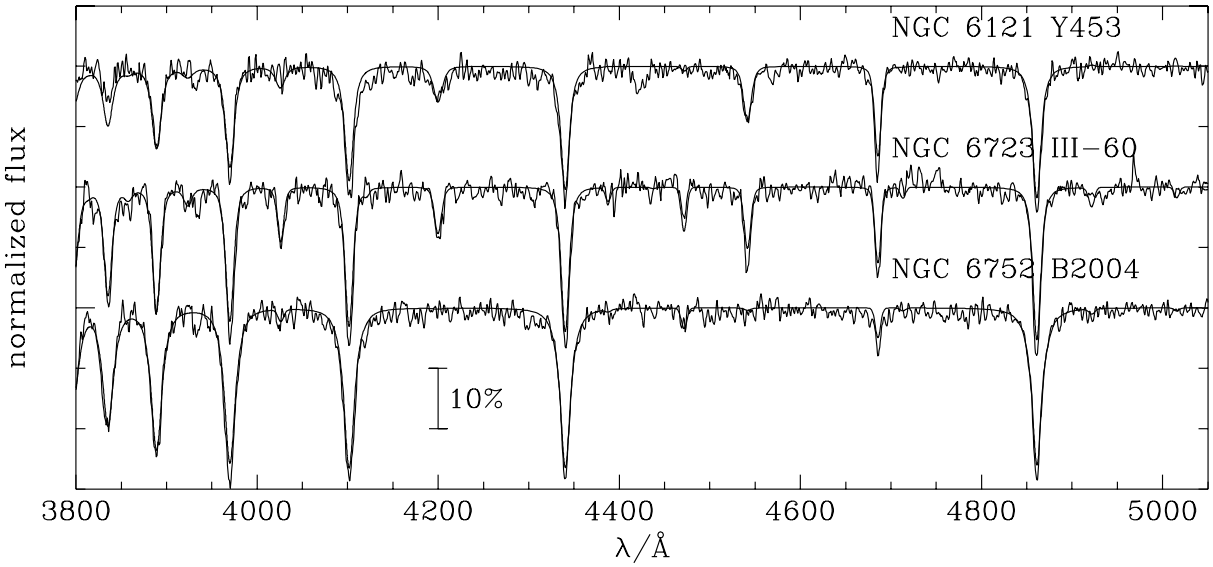

Fig. 2. The model atmosphere fits for the sdO stars.

Table 2. List of observed stars and their atmospheric parameters. The metallicities and radial velocities for the clusters are taken from the May 1997 tabulation of Harris (1996).

Cluster	[Fe/H]	$v_{hel,Cl.}$ [km/s]	Star	T_{eff} [K]	log g	$\log \frac{n_{He}}{n_H}$	v_{hel} [km/s]	M [$M_\odot$]	status	$\log\left(\frac{L}{L_\odot}\right)_{UV}$	$\log\left(\frac{L}{L_\odot}\right)_{V}$
NGC 2808	−1.37	+94	C2946	22700	4.48	−1.72	+93	0.46	post-EHB		+1.99
			C2947	15100	3.82	−1.21	+134	0.32	post-EHB		+1.78
			C4594	22700	4.06	−1.57	+89	0.55	post-EHB	+2.44	+2.41
NGC 6121	−1.20	+70	Y453	58800	5.15	−0.98	+31	0.16	post-EAGB	+2.61	+2.54
NGC 6723	−1.12	−95	III-60	40600	4.46	−1.03	−109	0.49	post-EAGB	+2.92	+3.06
			IV-9	20600	3.34	−0.83	−52	0.29	post-EAGB	+2.82	+2.79
NGC 6752	−1.55	−25	B2004	37000	5.25	−2.39	0	0.32	post-EHB	+1.94	+1.94

reddening toward M 4 (d = 1.73 kpc, E_{B-V} = 0.35) is taken from the HST study of Richer et al. (1997). We also use the nonstandard value of 3.8 for R_V [=A_V/E_{B-V}] toward M 4, as suggested recently by several authors (Peterson et al. 1995; Richer et al. 1997), along with the ISM parameterization of Cardelli et al. (1989).

Luminosities were determined by first using the distance and reddening to convert the V or UIT magnitude to an absolute magnitude, and then applying a bolometric correction using the T_{eff} derived from the model atmosphere fit. Because these hot stars have large bolometric corrections, the luminosities derived using the V magnitude are very sensitive to the value of T_{eff} ($\Delta \log L \sim 3\Delta \log T_{eff}$). The UIT magnitude has a much smaller bolometric correction, but typically has poorer photometric precision, and is more sensitive to reddening. Therefore, we have computed luminosities using both methods. As can be seen from Table 2 both values agree rather well. The uncertainty in the derived luminosities ranges from 0.12 dex for the cooler stars, to 0.16 dex to NGC 6121-Y453, assuming uncertainties of $0\overset{m}{.}1$ in V, $0\overset{m}{.}15$ in the UIT flux, $0\overset{m}{.}02$ in E_{B-V}, 0.035 dex in $\log T_{eff}$, and 10% in the cluster distances.

Knowing effective temperatures, surface gravities and absolute magnitudes we can derive the masses of the stars as described in Moehler et al. (1997). Assuming errors of $0\overset{m}{.}1$ and $0\overset{m}{.}13$ in the observed and theoretical V magnitudes, respectively, and 0.15 dex in $\log g$ we arrive at an error for log ($M/M_\odot$) of 0.18 dex or about 50%. For a detailed discussion of error sources see Moehler et al. (1997). The results are listed in Table 2.

6. Discussion

The derived effective temperatures and gravities of the target stars are plotted in Fig. 3, along with ZAHB and post-HB evolutionary tracks for [Fe/H] = −1.48 from Dorman et al. (1993), and post-AGB (0.565 $M_\odot$) and post-early AGB (0.546 $M_\odot$) tracks from Schönberner (1983). The stars NGC 6121-Y453, NGC 6723-III60, and NGC 6723-IV9 appear to fit the post-early AGB track, while the remaining four targets are consistent

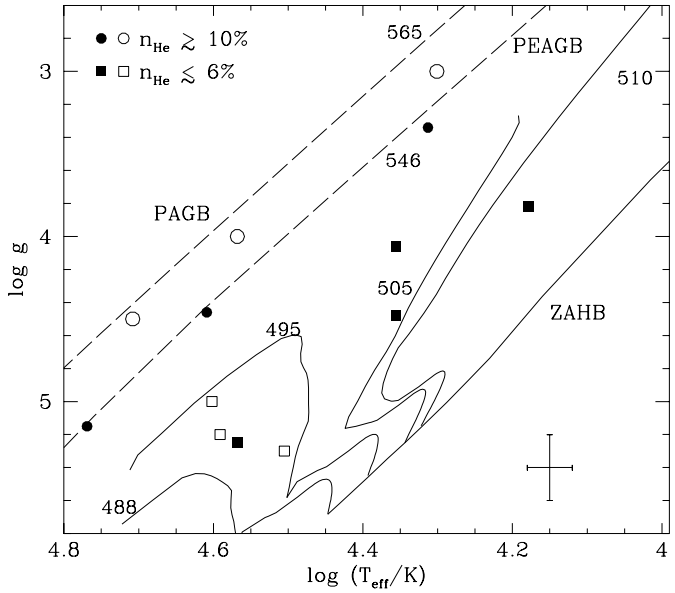

Fig. 3. The atmospheric parameters of the UV bright stars compared to evolutionary tracks. The solid lines mark the ZAHB and post-HB evolutionary tracks for [Fe/H] = −1.48 (labeled with the mass of the tracks in units of $10^{-3}\,M_\odot$, Dorman et al., 1993). The dashed lines give post-AGB (0.565 $M_\odot$) and post-early AGB (0.546 $M_\odot$) tracks from Schönberner (1983), also labeled with the mass of the tracks in units of $10^{-3}\,M_\odot$. The filled symbols are from this paper, the open symbols are taken from the literature (Conlon et al., 1994; Heber & Kudritzki, 1986; Heber et al., 1993; Moehler et al., 1997).

with post-EHB evolutionary tracks. In agreement with this scenario, the three post-early AGB stars have approximately solar helium abundances, while the post-EHB stars have subsolar helium abundances. The latter stars are expected to have subsolar helium abundances because they are direct descendants of EHB stars, which are known to show helium deficiencies (Moehler et al. 1997), most likely due to diffusion processes. The post-early AGB stars, on the other hand, have evolved off the AGB, where the convective atmosphere is expected to eliminate any previous abundance depletions caused by diffusion. Curiously, no helium-rich (He/H $\geq$ 1) sdO stars have yet been found in a globular cluster, although such stars dominate the field sdO population (Lemke et al. 1998).

As expected, the two clusters with a populous EHB (NGC 2808 and NGC 6752) have post-EHB stars but no post-AGB stars. The clusters NGC 6723 and M 4, on the other hand, do not have an EHB population, although they do have stars blueward of the RR Lyrae gap (which are potential progenitors of post-early AGB stars). The lack of true post-AGB stars may be understood from the different lifetimes: The lifetime of Schönberner's post-early AGB track is about 10 times longer than his lowest mass post-AGB track. Thus, even if only a small fraction of stars follow post-early AGB tracks, those stars may be more numerous than true post-AGB stars. Due to their relatively long lifetime, post-early AGB stars are unlikely to be observed as central stars of planetary nebulae (CSPNe) since any nebulosity is probably dispersed before the central star is hot enough to ionize it. Additional detail on the individual stars is given below.

6.1. NGC 2808

All three stars in NGC 2808 analysed in this paper are likely post-EHB stars. (Unfortunately, the best post-AGB candidate stars on the UIT image of NGC 2808 are too close to the cluster center to allow spectroscopy from the ground.) Although C2946 and C2947 could be separated in the long-slit optical spectra, they are too close together to estimate individual UV fluxes from the UIT image, and thus there is no UV luminosity determination in Table 2. Due to the well-populated EHB of NGC 2808 (Sosin et al., 1997), a large number of post-EHB stars are expected.

From their three-colour WFPC2 photometry of NGC 2808, Sosin et al. (1997) find a larger distance modulus [$(m\text{-}M)_0$ = 15.25 – 15.40] and lower reddening [E_{B-V} = 0.09 – 0.16] than the values adopted here from Harris (1996). The use of the distance and reddening of Sosin et al. would yield masses about 20% larger, and luminosities about 0.05 dex larger than the values given in Table 2.

6.2. NGC 6121 (M 4)

Y453 is possibly the hottest globular cluster star known so far. Other candidates are three central stars of planetary nebulae (IRAS 18333-2357 in M 22, Harrington & Paltoglou 1993; JaFu1 in Pal 6 and JaFu2 in NGC 6441, Jacoby et al., 1997), which however lack model atmosphere analyses of their stellar spectra. Such a high $T_{\rm eff}$ is not unexpected, since according to the Schönberner tracks, a post-AGB star will spend most of its lifetime at temperatures greater than 30,000 K. However, as pointed out by Renzini (1985), the large bolometric corrections of such hot stars in the visible have biased the discovery of post-AGB stars in favour of cooler stars.

In the $\log T_{\rm eff}$–$\log g$ plot, Y453 fits well on the 0.546 $M_\odot$ post-early AGB track of Schönberner (1983). However, our derived luminosity ($\log L/L_\odot$ = 2.6) is considerably lower than the Schönberner track at that $T_{\rm eff}$ and $\log g$, and the derived mass of 0.16 $M_\odot$ is astrophysically implausible. In order to obtain a mass of 0.55 $M_\odot$, the value of $\log g$ would need to be 5.68 instead of 5.15. This difference is too large to be accommodated by the spectral fitting, and still would not explain the discrepancy with the theoretically expected luminosity. Therefore, below we consider some other possible sources of error:

Line Blanketing: The use of fully line-blanketed NLTE models for the analysis of Y453 might result in a somewhat lower temperature (0.05 dex) without any changes in surface gravity (Lanz et al. 1997; Haas 1997). Such a lower temperature would increase the derived mass by about 15%.

Differential Reddening: Cudworth & Rees (1990) find a gradient in the reddening that would increase the adopted reddening for Y453 ($0^{\rm m}.35$) by about $0^{\rm m}.015$. Lyons et al. (1995) report a patchiness in the reddening toward M 4 that is at least as significant as the gradient, and find a total range

of 0.16 mag in E_{B-V}. An increase by such a large amount would still lead to a mass of only 0.3 $M_\odot$. Due to the non-standard reddening law toward M 4, the reddening correction for Y453 has a rather high uncertainty in any case.

Distance: The adopted distance (1.72 kpc) to M 4 is on the low side of the range of distance determinations but is supported by both a recent astrometric measurement (Rees 1996), and HST observations of the main-sequence (Richer et al. 1997). Use of the distance given by Harris (1996; 2200 pc) would give a mass of 0.26 $M_\odot$.

Photometry: The only ground-based photometry of Y453 of which we are aware is the photographic photometry of Cudworth & Rees (1990), who also derive a 99% probability of cluster membership from its proper motion. Y453 is among the faintest stars studied by Cudworth & Rees, so the photometric precision might be poorer than their quoted 0.025 mag (which corresponds to an error of 2% in M).

6.3. NGC 6723

The V and B−V magnitudes in Table 1 for III-60 are from Menzies (1974); we are not aware of any other photometry of this star. The tabulated photometry for IV-9 is from L.K. Fullton (1997, priv. comm.), who also gives U–B $= -0.84$. Photometry for IV-9 was also obtained by Menzies (1974; V = 14.86, B−V $= -0.25$), and Martins & Fraquelli (1987; V=14.69, B−V $= -0.142$). III-60 and IV-9 fit well on the 0.546 $M_\odot$ post-early AGB track (see above) of Schönberner, and also have luminosities ($\log L/L_\odot \sim 3.0$) consistent with being post-early AGB stars.

The spectrum of IV-9, however, was difficult to fit with any single model. As can be seen from Fig. 1 there is an absorption feature blueward of the He I line at 4713 Å, which matches the He II absorption line at 4686 Å in wavelength. The He II line strength and the Balmer line profiles can be reproduced by a model with $T_{\rm eff}$ = 30,000 K, $\log g$ = 4.08, and $\log \frac{n_{He}}{n_H}$ = −0.89. However, this model is inconsistent with both the size of the Balmer jump and with the photometric indices (optical and UV) of this star. The photometric data indicate a temperature of 20000 – 21000 K instead. Excluding the absorption feature at 4686 Å from the fit results in a temperature of 20700 K and a $\log g$ value of 3.34, in good agreement with the photometric temperature. The detection of metal lines (such as the O II absorption lines in BD+33°2642 discussed by Napiwotzki et al., 1993) could help to decide between the two temperatures. Simulations with theoretical spectra, however, show that due to the low resolution of our data we cannot expect to see any metal lines. Any decision will therefore have to await better data. We keep the cooler temperature for all further analysis because of the good agreement with the photometric indices.

6.4. NGC 6752

B2004 was one of only four post-EHB candidate stars present in the UIT color-magnitude diagram of NGC 6752 reported by Landsman et al. (1996), and the position of B2004 in the $\log T_{\rm eff}$–$\log g$ plot (Fig. 3) is consistent with post-EHB tracks. Landsman et al. estimated $T_{\rm eff}$ = 45000 K and $\log L/L_\odot$ = 2.12 for B2004 on the basis of IUE spectrophotometry. However, the IUE photometry of B2004 had large uncertainties due to the presence of the nearby ($2.5''$ distant) blue HB star B1995, and the $T_{\rm eff}$ (37000 K) and luminosity ($\log L/L_\odot$ = 1.94) of B2004 derived here should be more accurate. Spectroscopic analyses of the other three post-EHB candidate stars (B852, B1754, and B4380) in NGC 6752 were presented by Moehler et al. (1997). The four post-EHB stars in NGC 6752 occupy a fairly narrow range in temperature ($4.5 < \log T_{\rm eff} < 4.6$) and luminosity ($1.94 < \log L/L_\odot < 2.12$), and are separated by a large luminosity gap (0.5 dex) from stars on the populous EHB. As discussed by Landsman et al. (1996), these two characteristics are consistent with the non-canonical HB models of Sweigart (1997), which include helium mixing on the RGB. However, a more definitive test of EHB evolutionary tracks will require a larger sample of post-EHB stars.

7. Summary

Among the seven UIT-selected UV-bright stars observed in four globular clusters, we find three post-early AGB stars and four post-EHB stars, but no genuine post-AGB stars. This can be understood by different evolutionary time scales for these stages and by the HB morphology of the globular clusters observed: NGC 6752 shows only an almost vertical extended blue horizontal branch, which means that there is a lack of possible progenitors for post-AGB stars. In NGC 2808 the more luminous UV-bright stars could not be observed from the ground due to their proximity to the cluster center. The long blue tail of this cluster, on the other hand, provides plenty of progenitors for post-EHB stars. M 4 and NGC 6723 lack EHB stars - it is therefore no surprise that we do not find any post-EHB stars in these two clusters. The blue HB stars found in both clusters are potential progenitors of post-early AGB stars.

We find that post-EHB stars have sub-solar helium abundances, similar to their progenitors, which are identified with subdwarf B stars known in the field of the Milky Way, while the post-early AGB stars show more or less solar helium abundances. This difference is not unexpected, because the diffusive processes at work on the HB are counteracted by convection and mass loss on the AGB and afterwards.

The present results suggest that post-early AGB stars might be more numerous than post-AGB stars in globular clusters with a blue HB. Theoretical simulations would be useful to determine whether the relative populations of post-AGB and post-early AGB stars can be accommodated using existing post-HB evolutionary tracks. For example, in the models of Dorman et al. (1993), post-early AGB stars arise only from HB stars within a narrow temperature range near $\log T_{\rm eff} \sim 4.25$. However, any additional mass-loss processes, either on the hot HB or during the early AGB, would extend the $T_{\rm eff}$ range of the progenitors of post-early AGB stars to cooler HB stars. Such processes would also reduce the number of PN candidates and thereby reduce the discrepancy between the predicted and observed number of

PNe (Jacoby et al., 1997). Further study of the various globular cluster UV-bright stars (post-EHB, post-early AGB, and post-AGB) should provide important clues about the mass loss history of post-HB evolutionary phases.

Acknowledgements. SM acknowledges support by the Alexander von Humboldt-Foundation, by the director of STScI, Dr. R. Williams through a DDRF grant, and by the DARA through grant 50 OR 96029-ZA. Thanks go to Michael Lemke for the many model atmospheres, to Laura K. Fullton for supplying her photometry prior to publication, to Ben Dorman for valuable suggestions, and to the ESO staff for their support during the observations as well as afterwards. This research has made use of the SIMBAD data base, operated at CDS, Strasbourg, France.

References

Bergeron P., Saffer R.A., Liebert J., 1992, ApJ 394, 228
Brown T.M., Ferguson H.C., Davidsen A.F., Dorman B., 1997, ApJ 482, 685
Buonanno R., Caloi V., Castellani V., Corsi C.E., Fusi Pecci F., Gratton R., 1986, A&AS 66, 79
Cardelli J.A., Clayton G.C., Mathis J.S., 1989, ApJ 345, L245
Charlot S., Worthey G., Bressan A., 1996, ApJ 457, 625
Conlon E.S., Dufton P.L., Keenan F.P., 1994, A&A 290, 897
Cudworth K.M., Rees, R. 1990, AJ 99, 1491
de Boer, K.S. 1987, in The 2nd Conference on Faint Blue Stars, eds. A.G.D. Philip, D. Hayes, J. Liebert, (L. Davis Press, Schenectady), p. 95
Dixon R.I., Longmore A.J. 1993, MNRAS 265, 395
Dorman B., Rood R.T., O'Connell, R.W., 1993, ApJ 419, 596
Ferraro F.R., Clemintini G., Fusi Pecci F., Buonanno R., Alcaino G., 1990 A&AS 84, 59
Haas S., 1997, PhD thesis, University of Erlangen-Nürnberg, Germany
Hamuy M., Walker A.R., Suntzeff N.B., Gigoux P., Heathcote S.R., Phillips M.M., 1992, PASP 104, 533
Harrington J.P., Paltogou G. 1993, ApJ 411, L103
Harris W.E. 1996, AJ 112, 1487
Heber U., Kudritzki R.P., 1986, A&A 169, 244
Heber U., Dreizler S., Werner K., 1993, Acta Astron. 43, 337
Horne K., 1986, PASP 98, 609
Hummer D.G., Mihalas D., 1988 ApJ 331, 794
Jacoby G.H., Morse J. A., Fullton L.K., Kwitter K.B., Henry R.B.C, 1997, AJ 114, 2611
Landsman W.B., Sweigart A.V., Bohlin R.C., Neff S.G., O'Connell R.W., Roberts M.S., Smith A.M., Stecher T.P., 1996, ApJ 472, L93
Landsman W.B., Crotts A.P.S., Lanz T., Moehler S., Napiwotzki R., O'Connell R.W., Stecher T.P., Sweigart A.V., Whitney J.H. 1998, in preparation
Lanz T., Hubeny I., Heap S.R. 1997, ApJ 485, 843
Lemke M., Heber U., Napiwotzki R., Dreizler S., Engels D. 1998, Proceedings of the 3rd Conference on Faint Blue Stars, eds. A.G.D. Philip, J. Liebert, R.A. Saffer, D. Hayes, (L. Davis Press, Schenectady), in press
Lyons M.A., Bates B., Kemp S.N., Davies R.D. 1995, MNRAS 277 113
Martins D.H., Fraquelli D.A., 1987, ApJS 65, 83
Menzies J., 1974, MNRAS 168, 177
Moehler S., Heber U., Rupprecht G., 1997, A&A 319, 109
Napiwotzki R., 1997 A&A 322, 256
Napiwotzki R., Heber U., Köppen J., 1993, A&A 292, 239
Peterson R.C., Rees R.F., Cudworth K.M. 1995, ApJ 443, 124
Rees R. 1996, in Formation of the Galactic Halo . . . Inside and Out, ed. H. Morrison, A. Sarajedini, ASPC 92, 289
Renzini A., 1985, in Horizontal Branch and UV-Bright Stars, ed. A.G. Davis Phillip (Schenectady, L. Davis Press), 19
Richer H.B., Fahlmann G.G., Ibata R.A., Pryor C., Bell R.A., Bolte M., Bond H.E., Harris W.E., Hesser J.E., Holland S., Ivanans N., Mandushev G., Stetson P.B., Wood M.A., 1997, ApJ 484, 741
Saffer R.A., Bergeron P., Koester D., Liebert J., 1994, ApJ 432, 351
Savage B.D., Mathis F.S., 1979, ARAA 17, 73
Schönberner D., 1983, ApJ 272, 708
Sosin C. , Dorman B., Djorgovski S.G., Piotto G., Rich R.M., King I.R., Liebert J., Phinney E.S., Renzini A., 1997, ApJ 480, L35
Stecher T., Cornett R.H., Greason M.R., Landsman W.B., Hill J.K., Hill R.S., Bohlin R.C., Chen P.C., Collins N.R., Fanelli M.N., Hollis J.I., Neff S.G., O'Connell R.W., Offenberg J.D., Parise R.A., Parker J., Roberts M.S., Smith A.M., Waller W.H., 1997, PASP 109, 584
Sweigart A.V., 1997, ApJ 474, L23
Werner K. 1986 A&A 161, 177